

Characterization of Nonlinear Site Response Based on Strong Motion Records at K-NET and KiK-net Stations in the East of Japan



S. Noguchi & H. Sato

Central Research Institute of Electric Power Industry (CRIEPI), Abiko-shi, Japan

T. Sasatani

None, Sapporo-shi, Japan

SUMMARY:

We investigate the nonlinear soil response at various of seismic observation sites using strong motion observation data. We deal with a number of observation data at K-NET and KiK-net stations in Eastern Japan. We derive the nonlinear site characteristics at each station by means of DNL, a new quantitative index for nonlinear soil response based on observed data. We show that these nonlinear site characteristics can be categorized based on the linear site amplification characteristics; that is, the nonlinear soil response characteristics are similar if the linear response characteristics are similar. We discuss the relationship between these site characteristics and the soil parameters. Then we show the nonlinear soil response during the 2011 off the Pacific coast of Tohoku Earthquake using DNL. The changes of site response characteristics during and after the earthquake are shown very clearly by DNL.

Keywords: Nonlinear Site Response, Strong Motion Record, 2011 off the Pacific coast of Tohoku Earthquake

1. INTRODUCTION

After the installation of dense strong motion observation network K-NET and KiK-net by NIED in Japan, it becomes clear that the nonlinear soil response, which is already well known phenomenon in soil mechanics, occurs frequently during strong shaking. In case of strong motion whose peak ground acceleration (PGA) exceeds 100 cm/s^2 , the nonlinear soil response affects especially high frequency motion. It could induce serious misfit between the simulated and observed accelerations (ex. Sasatani *et al.*, 2008).

To consider such nonlinear soil response, usually, the nonlinear analysis like equivalent linear method is conducted. Yet, it is difficult actually to apply such method to data at hundreds of stations, like the accumulated thousands of waveforms observed by K-NET and KiK-net. In addition, these analysis require some soil parameters. However, it is often difficult to derive enough soil parameters for such nonlinear analysis. In this condition, we proposed a new quantitative index for nonlinear soil response, DNL (Degree of Non-Linearity, Noguchi and Sasatani, 2008; Noguchi and Sasatani, 2011).

In this paper, we show the nonlinear soil response characteristics at some stations using seismic observation data only, by means of DNL. We categorize these stations in terms linear and nonlinear site characteristics, and discuss the relationship between these characteristics and soil parameters. Then we show the nonlinear soil response during 2011 off the Pacific coast of Tohoku Earthquake (Mw 9.0) utilizing DNL. We focus on the change of nonlinear soil response over time during and after the mainshock.

2. THE QUANTITATIVE INDEX FOR NONLINEAR SOIL RESPONSE

In this section, we describe the quantitative index for nonlinear soil response based on strong motion record, DNL. Then, we introduce the “nonlinear site characteristics” at an observation station, which is expressed using DNL.

2.1. The Definition of the Index for Nonlinear Soil Response

The DNL is a new index for nonlinear soil response based on the strong motion data. To deal with hundreds of strong motion data, the DNL is designed to be calculated easily and almost automatically. It also does not need any soil parameter. The DNL is calculated using the change of spectral ratios due to nonlinear soil response. It is already well known that when nonlinear soil response occurs, the surface to borehole spectral ratio for S-wave horizontal motion (Surface/Borehole spectral ratio hereafter), which represents the soil response characteristics for S-wave, shows typical changes (ex. Beresnev and Wen, 1996). Namely, the dominant peak shifts lower frequency and the amplification at high frequency decreases. The Surface/Borehole spectral ratio usually used in analysis for nonlinear soil response can be utilized for DNL. In addition, S-H/V spectral ratio, the S-wave horizontal to vertical spectral ratio at surface, is also available for DNL. Wen *et al.* (2006) reported that the S-H/V spectral ratio also changes in case of nonlinear soil response. If we use the S-H/V spectral ratio, we do not need any borehole or rock site record to derive DNL.

The DNL is simply defined as a summation of the gap between the target spectral ratio during strong motion and that for the reference as below;

$$\text{DNL} = \sum \left| \log \left(\frac{R_{\text{Target}}(f)}{R_{\text{Reference}}(f)} \right) \right| \Delta f \quad (1)$$

In the equation (1), the R_{Target} means Surface/Borehole or S-H/V spectral ratio for strong motion data which is suspicious of nonlinear soil response. The $R_{\text{Reference}}$ means the reference spectral ratio which is made from weak motion records which represent almost linear soil response. Δf is frequency interval. In this paper, the frequency range of this summation is set from 0.5 to 20 Hz for all data. It is because we process a huge number of data at a variety of sites almost automatically. This DNL value also can be represented as shown in Fig. 1. It is important that the DNL mainly depends on the gap at high frequency, that is, more than a half of DNL value is determined by the gap between 10 and 20 Hz. Similar indexes for nonlinear soil response using the change of spectral ratio also have been proposed (Hartzell, 1998; Wen *et al.*, 2006). The uniqueness of our DNL is to deal with wide frequency range uniformly among some stations. We name the DNL derived from Surface/Borehole spectral ratio DNL_{SB} and DNL for S-H/V spectral ratio DNL_{HV} .

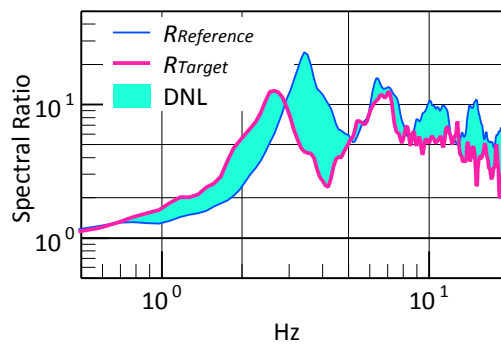


Figure 1. Schematic figure of DNL. The coloured area corresponds to the summation value in equation (1).

In this paper, to derive these spectral ratios, we apply a simple way on all waveform data. It is because we aim to process a huge amounts of data almost automatically. To calculate the target spectral ratio, first we derive Fourier amplitude spectra using the S-wave portion from each components of strong motion data. The time windows for all components, horizontal, vertical, surface and borehole are the same, and applied 10 % cosine taper on the both side of the window. Then we derive the horizontal amplitude spectrum as a geometric mean of spectra from two horizontal components. The

Surface/Borehole spectral ratio is derived by dividing the horizontal amplitude spectrum at surface by that for the borehole records. Similarly, the S-H/V spectral ratio is derived by dividing the horizontal amplitude spectrum at surface by that for the vertical component at surface. The length of time window is basically 10.24 s, but determined to cover all the S-wave portion. To make the reference spectral ratios representing linear soil response, we choose 3~10 set of weak motion ($<50 \text{ cm/s}^2$) record at each station. The reference spectral ratio is the geometric mean of these spectral ratios for weak motion.

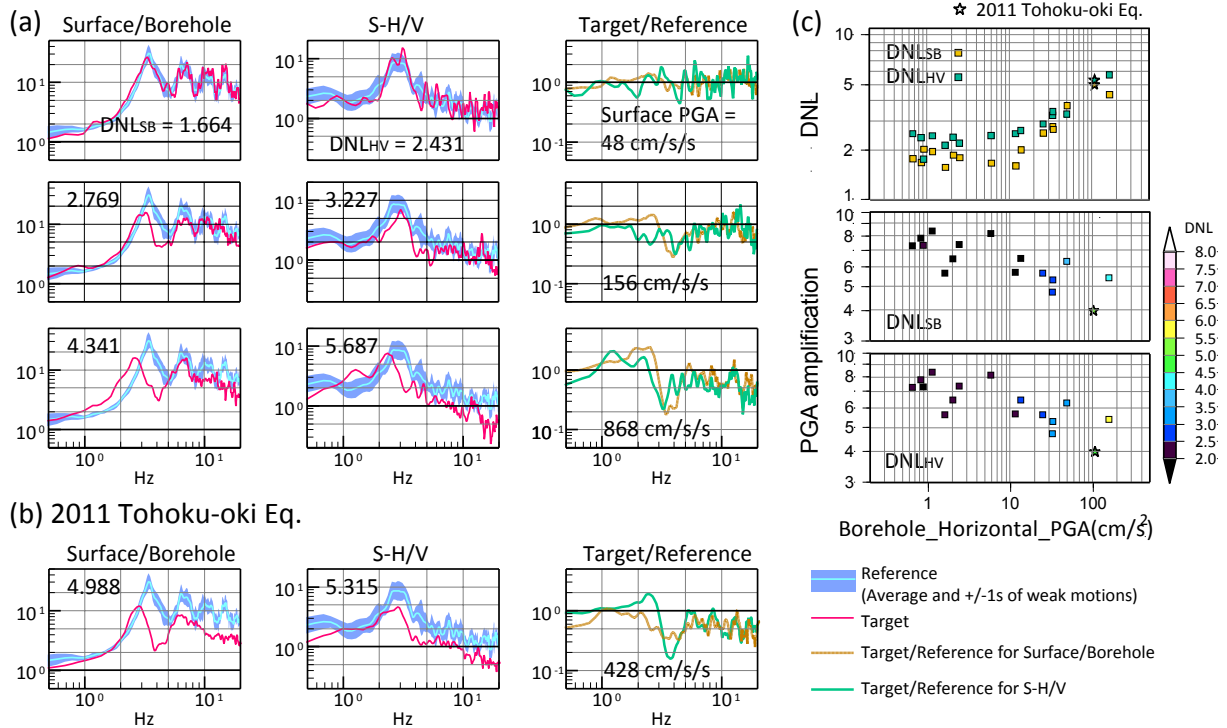


Figure 2. Spectral ratios and DNL values at KiK-net vertical array station IWTH04. (a) Comparison of spectral ratios for some observations. (b) Spectral ratios for the 2011 Tohoku-oki Earthquake. (c) DNL values vs. borehole PGA and PGA amplification vs. borehole PGA.

2.3. The Site Characteristics based on Strong Motion Record Expressed by DNL

In Fig. 2 (a) and (b), we show some examples of DNL values for KiK-net vertical array strong motion observation station IWTH04. We can see that the Surface/Borehole and S-H/V spectral ratios change gradually as the acceleration amplitude at surface rises. As these typical changes, we can recognize that these changes are due to nonlinear soil response. In the right hand of Fig. 2 (a) and (b), the Target/Reference spectral ratios are shown, which is the spectral ratio for target Surface/Borehole or S-H/V spectral ratio shown as red line to the references shown as blue line. This comparison shows clearly that the change of S-H/V spectral ratio is quite similar to that for Surface/Borehole spectral ratio. It indicates that the S-H/V spectral ratio also changes due to nonlinear soil response, similar to the Surface/Borehole spectral ratio.

These changes of spectral ratios make the DNL values larger as the ground motion level rises. This tendency is shown clearly in Fig. 2 (c). Both DNL values do not become smaller than around 2. It is because the spectral ratios for observed data has some fluctuation even for weak motion that linear response is expected. If the acceleration level at borehole exceeds $\sim 20 \text{ cm/s}^2$ ($\sim 100 \text{ cm/s}^2$ at surface), the DNL values rise as shown in Fig. 2 (a). At the same time, the PGA amplification decreases because of nonlinear soil response.

It can be considered that these tendencies for DNL, PGA and PGA amplification relationships

represent the characteristics of nonlinear soil response at the station. These relationships are alike with dynamic deformation characteristic in the way that it also represents the relationship between the degree of nonlinear soil response and ground motion strength. It is important that the nonlinear soil characteristics shown in Fig. 2 (c) is derived without any soil parameters. In addition, The DNL_{HV} does not need any borehole record. Thus, by means of DNL_{HV} , we can derive the characteristic of nonlinear soil response from 3-components of strong motion data only.

3. THE CATEGORIES OF NONLINEAR SITE CHARACTERISTICS

We investigate the relationship between nonlinear site characteristics expressed by DNL and the other site characteristics, the soil parameters derived by PS-logging at a number of strong motion stations. We find out that these stations can be categorized into some types based on these linear and nonlinear site characteristics.

In Fig. 3, 3 categories of site characteristics are shown. They are categorized in terms of the types of linear soil amplification characteristics (shown by blue lines). The category 1 (Fig. 3 (a)) stations have no significant peak for soil amplification. They are all located at Kitakami Mountains which consists of hard bedrocks older than the Mesozoic. The PGA amplifications are also smaller compared to the other categories, being almost independent of borehole PGA. At these stations, the spectral ratios do not change so much even with the strong motion, so DNL_{SB} also do not rise so much. In such stations, it can be said that the nonlinear soil response hardly occurs.

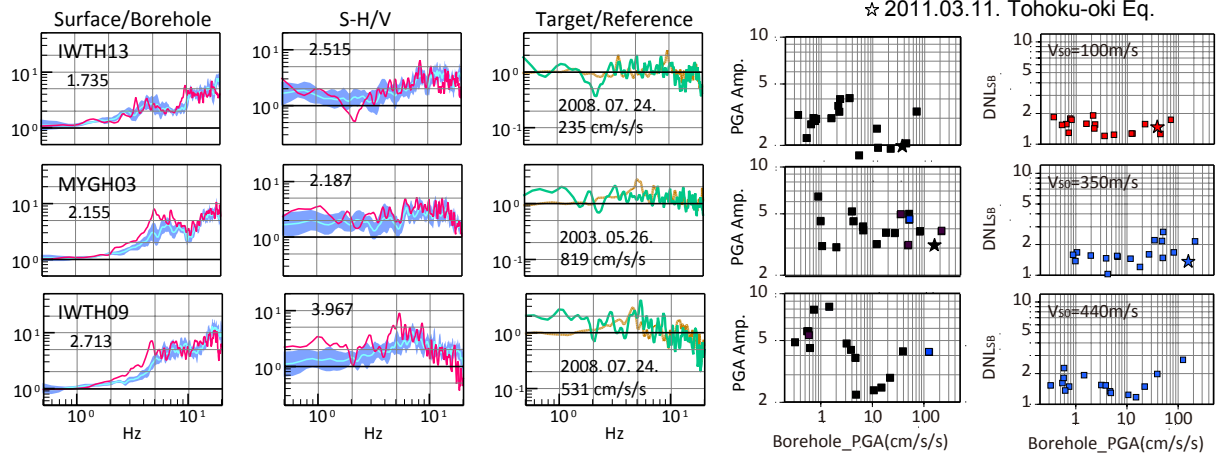
For category 2 (Fig. 3 (b)), the stations have a broad peak of amplification in Surface/Borehole spectral ratios. The shapes of S-H/V spectral ratios for these stations are also similar. Interestingly, these spectral ratios also show quite similar changes for the strong motion. Because of it, the tendencies of DNL_{SB} rising as the input PGA are also similar. At the same time, the decrease of PGA amplifications with the increase of input PGA are also comparable. Many of such type of stations are located on highly weathered granite or volcanic locks, where the S-wave velocity derived by PS-logging rises gradually as it goes deeper .

The category 3 (Fig. 3 (c)) stations are characterized by very sharp peak of amplification in Surface/Borehole spectral ratio. It would be attributed to a few meters of surface soil layer they all have. The changes of spectral ratios in this category are also quite similar, as we found in other categories. The stations in this category can be characterized by large value of DNL_{SB} for strong motion.

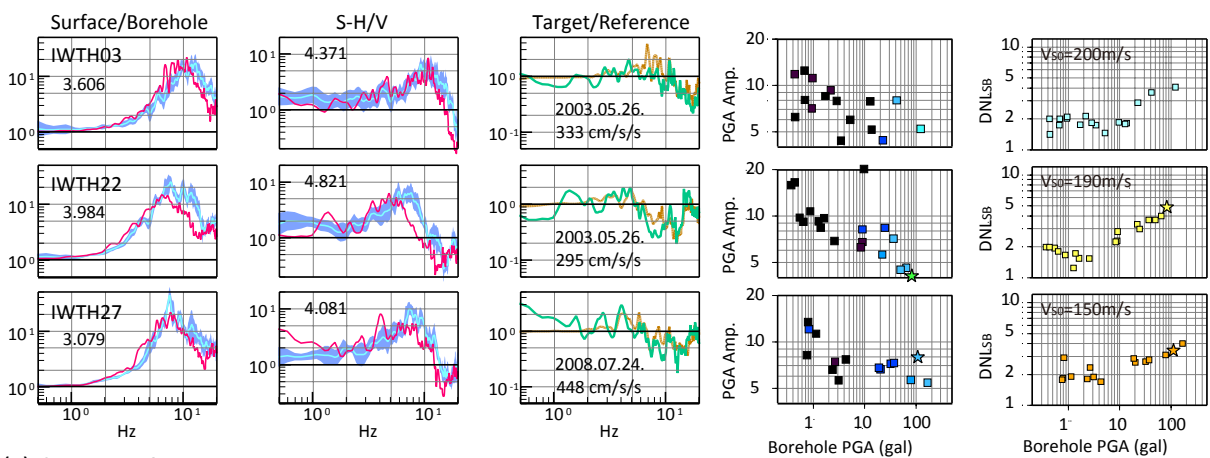
From these comparison, it is shown that the changes of spectral ratios due to nonlinear soil response are similar if the linear site amplification characteristics also similar. Therefore, the nonlinear site characteristics expressed by DNL_{SB} are also similar in each categories. Furthermore, these characteristics also related to the decline of PGA amplification due to nonlinear soil response. Utilizing these empirical relationships, it could be possible to estimate the nonlinear soil behaviour and the decline of PGA amplification at other stations, even the station has no experience of nonlinear soil response. As shown above, these relationships also can be represented using DNL_{HV} , without borehole records.

We can expect that these characteristics of nonlinear soil response can be related to the soil properties. In Fig. 3, V_{S0} , the S-wave velocity of uppermost soil layer at the station are also shown. Although we cannot find any dependency of nonlinear characteristic on V_{S0} among these examples. Due to the logging data by NIED, the soil types at these stations are quite vary, that is, clay, sand, gravel and so on. It seems that the number of examples in each category are possible to be insufficient to find out a relationship, however the uncertainty of V_S estimated by PS-logging might be responsible.

(a) Category 1



(b) Category 2



(c) Category 3

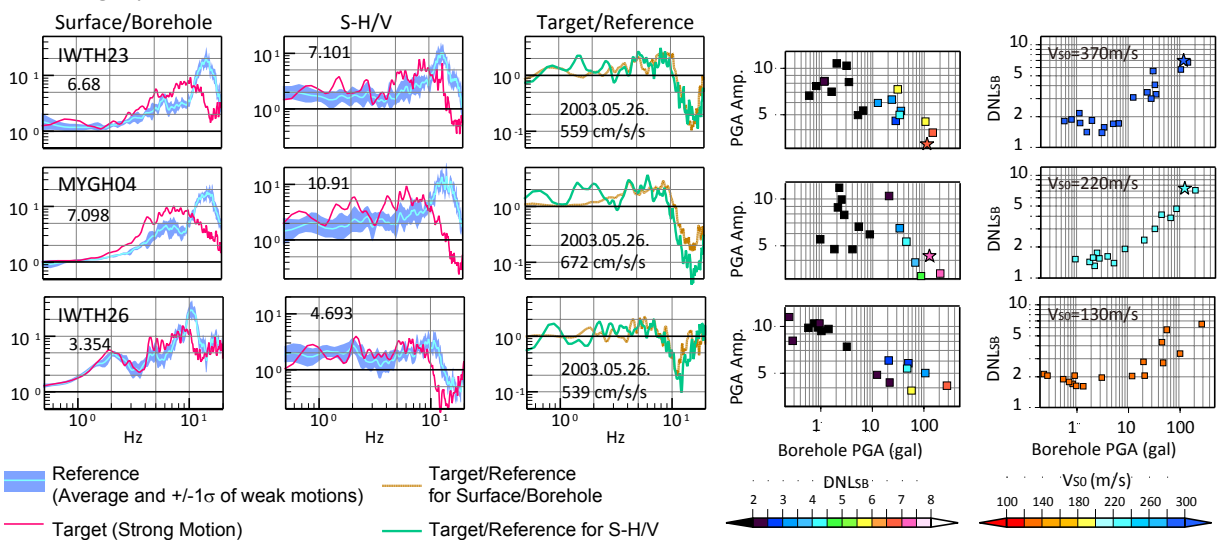


Figure 3. Three categories of nonlinear site characteristics for KiK-net borehole stations.

4. NONLINEAR SOIL RESPONSE DURING 2011 TOHOKU-OKI EARTHQUAKE

The 2011 off the Pacific coast of Tohoku Earthquake (Mw 9.0, Tohoku-oki Earthquake hereafter) induced strong motion over wide area in Eastern Japan. During this huge earthquake, strong shaking over 1000 cm/s^2 were observed at 19 stations of K-NET and KiK-net. The strong ground motion also

lasted for a long time (100 s or more) at many stations (ex. Furumura *et al.*, 2011). In this section, we investigate the nonlinear soil response during the Tohoku-oki Earthquake based on strong motion record utilizing DNL.

4.1. Nonlinear Soil Response during 2011 Tohoku Earthquake in terms of DNL

Fig. 2 (b) shows the spectral ratios during Tohoku-oki Earthquake at IWTH04 vertical array. Although the time window for spectral ratios is much longer (163.84 s), The changes of these spectral ratios are similar to the other case shown in Fig. 2 (a). Also, the relationship between PGA, DNLs and PGA amplification (stars in Fig.2 (c)) are not particular compared to the other. The DNL values during Tohoku-oki Earthquake at the other stations are shown by stars in the right panels in Fig. 3. Similar to IWTH04, the nonlinear soil response expressed by DNL are not particular so much, so to say, in usual even though the long duration of strong motion due to the huge earthquake.

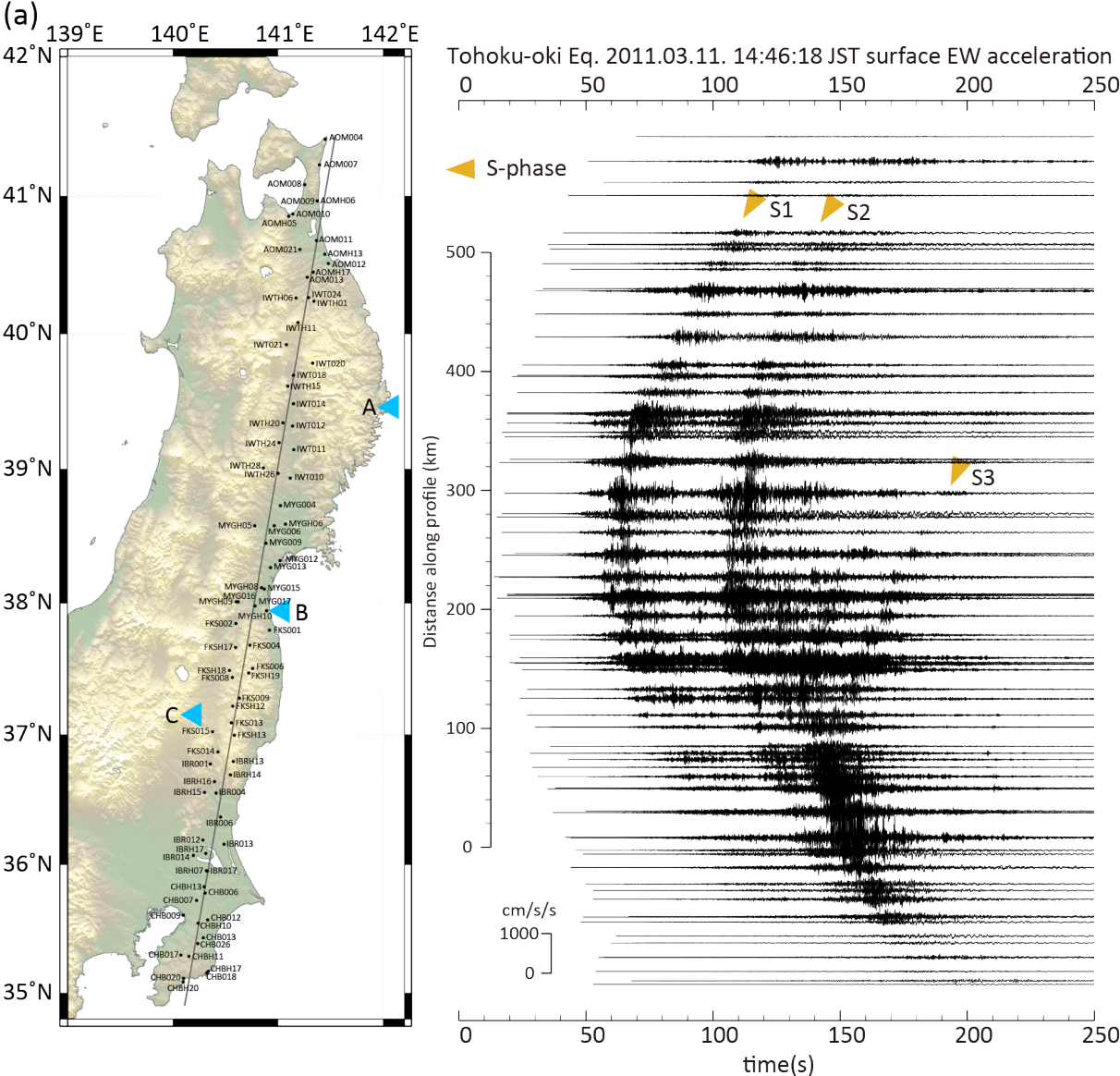


Figure 4. Nonlinear soil response at KiK-net stations during the 2011 Tohoku-oki Earthquake. (a) Strong motions records during the Tohoku-oki Earthquake. A, B, and C are the stations shown in (b). (b) Change of spectral ratios and DNLs over time based on running spectra.

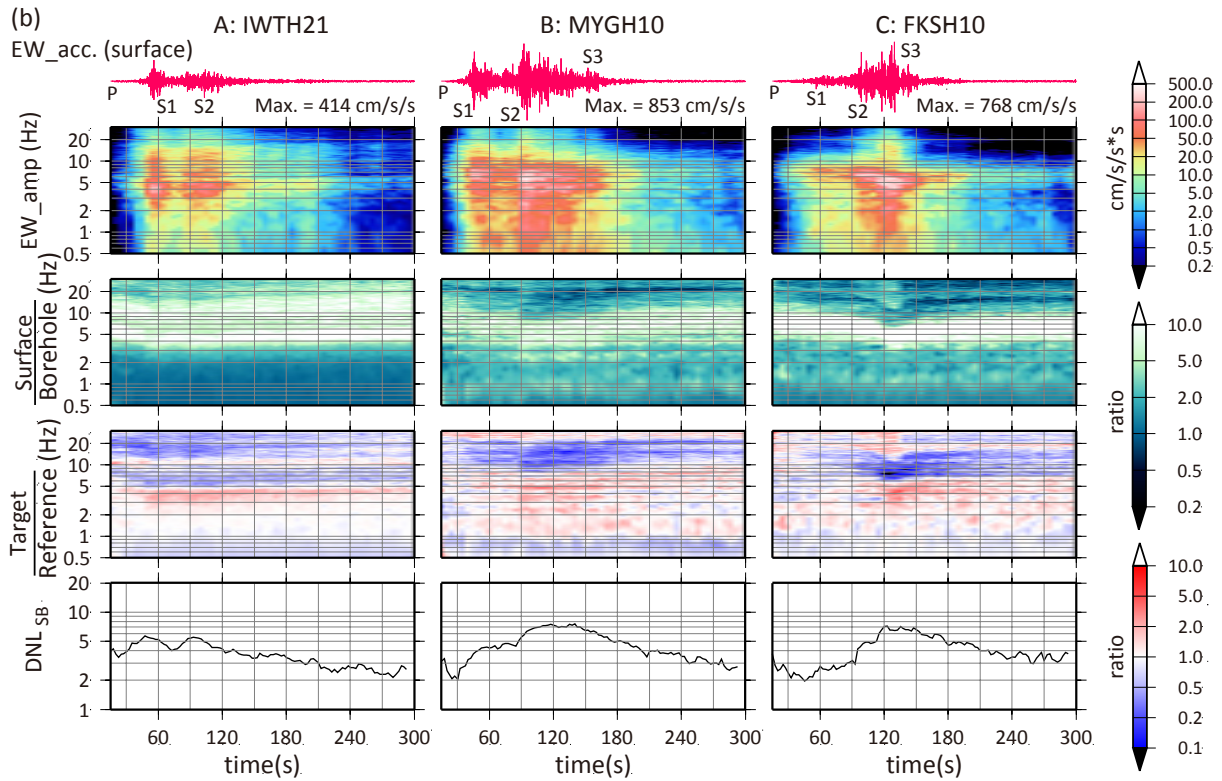


Figure 4. (continued)

4.2. The Change of Site Response Characteristics during and after Tohoku-oki Earthquake

To investigate the change of nonlinear soil response during strong motion lasted for a long time, we calculate Surface/Borehole spectral ratios and their DNL_{SB} using running spectra. The 10.24 s of time windows are picked up shifting the start of the window with the step of 2.5 s from the start to the end of the record. For each window, the Fourier amplitude spectra, Surface/Borehole spectral ratios, their Target/Reference spectral ratios and DNL_{SB} are calculated in the same way mentioned in Section 2.

The result for 3 KiK-net stations are shown in Fig. 4. The strong motion observed during Tohoku-oki Earthquake (Fig. 4 (a)) are characterized by long-lasting complicated waveforms reflecting the complex source process. We can find at least 3 main S-phases (S1-S3) in waveform paste-up shown in Fig. 4 (a). We choose 3 typical stations (A-C) shown in the location map which have unique waveforms individually.

The running spectra, spectral ratios and DNL_{SB} at these stations are shown in Fig.4 (b). First, we should be sure whether the Surface/Borehole spectral ratios are governed mainly by the S-wave multiple reflection in surface layer or not. It is because the reference spectral ratio for Target/Reference spectral ratio represents the linear soil response.

The data shown in Fig. 4 (b) are all start just as the P-wave incident. The S-wave incidents after several tens of seconds after P-wave. After the S-wave incident, Surface/Borehole spectral ratios seem to keep similar form (peaks and troughs) showing typical changes due to nonlinear soil response, that is, the shift of dominant peak and the decline of amplification at high frequency. The Target/Reference spectral ratios are also show that the S-wave multiple reflection is dominant after the S-wave incident. In fact, just after the S-wave incident (~ 50 s), The Target/Reference spectral ratios are almost flat in 1 compared to the before and after parts. After that, they seem to show the change due to nonlinear soil response. So we can say that the general shapes of Surface/Borehole spectral ratios lasting through the record are governed mainly by the S-wave multiple reflection in surface layer representing the S-wave response characteristics.

In Fig. 4 (b), we can see that the Surface/Borehole spectral ratios show typical changes of nonlinear soil response immediately just as the strong motion incidents at all stations. The changes of Target/Reference spectral ratios indicate that these changes recover and close in the reference immediately (tens to hundreds of seconds after strong shaking), but a part of their decline (blue area) remains until the end of the record especially at high frequency. Such tendencies of these spectral ratios also appeared commonly at the other stations which hit by strong shaking during Tohoku-oki Earthquake. We can see that the DNL_{SB} reflects these changes of site response very clearly. They reflect the change of S-wave response characteristics due to nonlinear soil response induced by long and unique ground motions at each stations very well.

4.3. The Long Term Change of Site Response Characteristics after Tohoku-oki Earthquake

During the Tohoku-oki Earthquake, the cyclic mobility waveforms were recorded at 6 K-NET stations and 1 KiK-net vertical array station. The KiK-net station FKSH14, one of such stations, is located at several hundred meters from sand beach in Fukushima, and has 21 m deep sand layer at surface. Fig. 5 (a) shows cyclic mobility waveform at around 110-130 s. We can expect that the site response characteristics at such stations would change in long term (several months or more) due to severe ground motion.

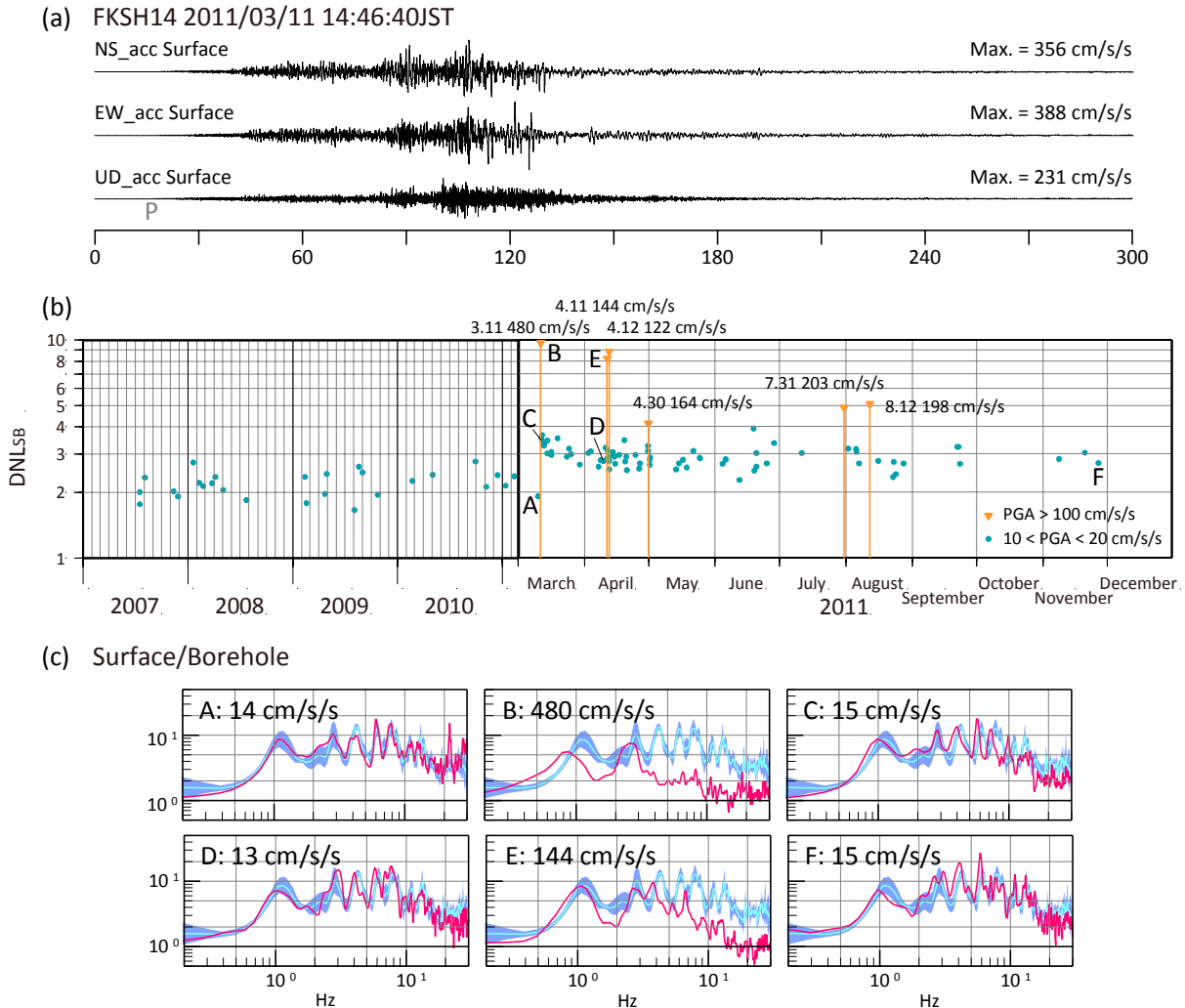


Figure 5. Long term change of site response at KiK-net FKSH14 before and after the Tohoku-oki Earthquake. (a) Acceleration waveforms at surface of FKSH14 during the Tohoku-oki Earthquake. (b) Change of DNL_{SB} at FKSH14 for strong and weak motions. (c) Surface/Borehole spectral ratios for some records indicated in (b).

In Fig. 5 (b), the DNL_{SB} values for weak and strong motions at FKSH14, before and after the Tohoku-oki Earthquake, are shown. The DNL_{SB} for mainshock of Tohoku-oki Earthquake is marked in B. The quite large value is reasonable because the site response characteristics should change dramatically during cyclic mobility. Importantly, it is shown significantly that the DNL_{SB} for weak motions became larger after the cyclic mobility. In Fig. 5 (c), the Surface/Borehole spectral ratios for some records are shown. For the record C, several hours after the mainshock, the amplification at high frequency is still smaller. We can see that the decline of amplification makes the DNL_{SB} value larger. The change remains at D, a month after the mainshock. Even for the strong motion E, the DNL_{SB} is larger compared to later strong motions. After around 8 months, as shown in F, the DNL_{SB} still larger compared to before the mainshock. In the Surface/Borehole spectral ratio for F, the amplification at high frequency (> 15 Hz) still slightly smaller than the reference.

These processes indicate that the site response characteristics at FKSH14 changes after cyclic mobility in both strong and weak motions, then it recovers very slowly not yet completely. The long term change of site response characteristics due to severe ground motion has reported in terms of the lower shift of dominant peak (ex. Sawasaki *et al.*, 2006). We show our own result by means of DNL, that is, the long term change of site response characteristic focussing on the decline of soil amplification at high frequency.

5. CONCLUSION

We investigated the nonlinear soil response characteristics at a number of strong motion station based on ground motion observation data, using the new method DNL. We found that the nonlinear site characteristics expressed by DNL based on the observation data can be categorized in terms of linear and nonlinear site amplification characteristics. We showed that the nonlinear soil characteristics are similar in each category, and could be applied for the estimation of nonlinear soil response at the site which has similar site characteristics.

We also showed the nonlinear soil response occurred during the 2011 Tohoku-oki Earthquake (Mw 9.0). Despite of the long duration, the nonlinear soil response appeared in the spectral ratio and DNLs are not so particular compared to the cases for the other earthquakes. It was shown clearly that the site response changes dramatically just as the strong motion incidence, and recovers immediately. Yet it was also shown that a part of the change of site response remained over several months by means of DNL. These results also showed that the DNL is quite useful to express the nonlinear soil response very clearly and easily.

After the 2011 Tohoku-oki Earthquake, a huge number of strong motion records over 100 cm/s^2 were recorded widely in Eastern Japan. Now we can utilize these data to derive a variety of nonlinear soil response characteristics, and make them a base to derive an empirical site characteristics considering nonlinear soil response.

ACKNOWLEDGEMENT

We used the strong motion data recorded by K-NET and KiK-net (<http://www.kyoshin.bosai.go.jp/kyoshin/>) installed by National Research Institute for Earth Science and Disaster Prevention (NIED) and logging data at KiK-net stations.

REFERENCES

- Beresnev, I. A. and Wen, K. L. (1996). Nonlinear Soil Response -- A Reality?, *Bulletin of the Seismological Society of America*, **86:6**, 1964–1978.
- Furumura, T., Takemura, S., Noguchi, S., Takemoto, T., Maeda, T., Iwai, K. and Padhy, S. (2011). Strong ground motions from the 2011 off the pacific coast of Tohoku, Japan (Mw=9.0) earthquake obtained from a

- dense nation-wide seismic network, *Landslides*, **8:3**, 333-338.
- Hartzell, S. (1998). Variability in nonlinear sediment response during the 1994 Northridge, California, earthquake. *Bulletin of the Seismological Society of America*, **88:6**, 1426–1437.
- Noguchi, S. and Sasatani, T. (2008). Quantification of degree of nonlinear site response, *14th World Conference on Earthquake Engineering*, 03-03-0049.
- Noguchi, S. and Sasatani, T. (2011). Nonlinear soil response and its effects on strong ground motions during the 2003 Miyagi-Oki intraslab earthquake, *Zisin 2*, **63:3**, 165-187 (in Japanese with English abstract).
- Sasatani, T., Noguchi, S., Maeda, T. and Morikawa, N. (2008). Recipe for predicting strong ground motions from future large intraslab earthquakes, *14th World Conference on Earthquake Engineering*, 03-01-0023.
- Sawasaki K., Sato, H., Nakahara, H. and Nishimura, T. (2006). Temporal change in site response caused by earthquake strong motion as revealed from coda spectral ratio measurement, *Geophysical Research Letters*, **33**, L21303.
- Wen, K. L., Chang, T. M., Lin, C. M. and Chiang, H. J. (2006). Identification of nonlinear site response during the 1999, Chi-Chi, Taiwan earthquake from the H/V spectral ratio. *3rd International Symposium on the Effects of Surface Geology on Seismic Motion*, **No. 012**, 225–232.